Metabolic network construction reveals probiotic-specific colonization resistance in a synthetic small intestinal community

Jack Jansma [1], Anastasia Chrysovalantou Chatziioannou [1*], Kitty Castricum [2], Saskia van Hemert [2], Sahar El Aidy [1#]

Affiliations

[1] Host-microbe Interactions, Groningen Biomolecular Sciences and Biotechnology Institute (GBB), University of Groningen, Groningen, The Netherlands.

[2] Winclove Probiotics, Amsterdam, the Netherlands

*Present address: Department of Chemistry, Laboratory of Analytical Biochemistry, University of Crete, Heraklion, Greece

[#] Corresponding author

Sahar El Aidy. Host-microbe Interactions, Groningen Biomolecular Sciences and Biotechnology Institute (GBB), University of Groningen, Nijenborgh 7, 9747 AG Groningen, The Netherlands. P: +31(0)503632201.

E: sahar.elaidy@rug.nl

Abstract

The gut microbiota plays a crucial role in maintaining overall health and probiotics have emerged as a promising microbiota-targeted therapy for improving human health. However, the molecular mechanisms of probiotics action in general and the targeting of small intestinal microbiota by probiotics are not well understood. To address this, we constructed a synthetic community of three species, which resembles the upper small intestinal microbiota. Our results indicate that probiotic supplementation can directly affect the metabolism of the community, resulting in colonization resistance in a probiotic specific manner. Supplementation with *Streptococcus thermophilus* led to increased lactate production and a decrease in pH, while *Lactobacillus casei* supplementation increased the resistance to perturbations and nutrient utilization without affecting lactate production or pH. Additionally, when combined with kynurenine, *Lactobacillus casei* enhanced the kynurenine pathway metabolism resulting in elevated kynurenic acid levels and possibly indirect colonization resistance. Overall, our study reveals how selecting probiotics with distinct functional capacities can unlock the full potential of microbiota-targeted therapies.

Keywords

Small intestine, microbiota, probiotics, dynamic metabolic networks, kynurenic acid

53

54 **Introduction**

55 In recent decades, there has been a growing interest in investigating the gut-microbiota and its
56 significant roles in maintaining human health [1, 2]. The gut-microbiota is composed primarily of
57 *Bacteroidaceae*, *Prevotellaceae*, *Rikenellaceae*, *Lachnospiraceae* and *Ruminococcaceae*, which reside
58 mainly in the colon [3]. In contrast to the colon, the small intestinal microbiota is highly dynamic and
59 location-specific. For example, *Streptococcaceae* and *Veilonellaceae* are abundant in the duodenum
60 [4], while *Streptococcaceae*, *Carnobacteriaceae* and *Actinomycetaceae* prevail in the jejunum [5] and
61 *Lactobacillaceae*, *Erysipelottrichaceae*, and *Enterobacteriaceae* are dominant in the ileum [6]. The
62 small intestinal microbiota plays a crucial role in regulating the metabolic, endocrine, and immune
63 functions of their hosts [7–9]. Consequently, altering the equilibrium between the host and the
64 microbiota can negatively affect the health of the host [10, 11]. Thus, to re-establish this equilibrium
65 and enhance the health of the host, multiple microbiota-targeted therapies, such as probiotics, are
66 employed [12].

67 Probiotics are defined as live microorganisms that, when administered in adequate amounts, confer
68 a health benefit on the host [13]. The development of probiotic therapies aiming at targeting the
69 small intestinal microbiota poses a significant challenge due to the limited access to the human small
70 intestine. Currently, investigations into the effect of probiotics on the small intestine are carried out
71 either directly on animal models [9, 14] or indirectly through small clinical trials that lack detailed
72 molecular mechanisms [15]. This lack of understanding hampers the development of novel probiotic
73 therapies. In recent years, it has been demonstrated that the microbiota retrieved from stoma
74 effluent exhibits similar compositional and behavioral characteristics with the healthy ileal
75 microbiota [16]. These findings suggest that the stoma effluent-derived microbiota may serve as a
76 promising source for probiotic research [17, 18]. However, the utilization of stoma effluent is limited
77 for the study of the upper small intestine. To address this limitation, there is a need for construction
78 of synthetic bacterial communities to bridge this research gap [19]. Synthetic bacterial communities

are bacterial mixtures produced through co-culturing of selected bacteria in controlled environments [20]. These communities can comprise a range from two [21] to over one hundred species [22]. Synthetic communities can be subjected to perturbation through manipulation of growth parameters or the introduction of new bacterial species, and can also be supplemented with specific compounds such as prebiotics [23]. Analysis of the community's molecular response allows a deeper understanding of the underlying molecular mechanisms [24], optimization of metabolites' production [25] and assessment of emergent properties such as stability or resistance to perturbations [26, 27]. This methodology has the potential to guide the development of novel microbiota-targeted therapies.

In humans, the kynurenine pathway is the primary route for the metabolism of free tryptophan, and it plays a critical role in the generation of energy in the form of nicotinamide adenine dinucleotide (NAD^+), immune system regulation [28] and the production of the neuroactive compounds quinolinic and kynurenic acid (KYNA) [29]. Increased tryptophan metabolism via the kynurenine pathway in the gut is associated with obesity and alterations in the microbiota [29]. G-protein coupled receptor 35 (GPR35), which is activated by KYNA, is abundantly expressed in the intestine, where it plays a role in immune regulation and epithelial barrier function [30]. The concentration of KYNA in the gut lumen increases from the proximal to the distal part of the intestine, indicating production by the gut microbiota [31, 32]. Several gut bacteria can produce compounds from the kynurenine pathway [32, 33] and probiotics supplementation have been shown to reduce intestinal inflammation and improve intestinal barrier function accompanied by reduced kynurenine but increased KYNA levels [34, 35]. However, the precise effects of kynurenine pathway metabolism within the microbiota remain unknown.

In the present study, a dynamic correlation-based network approach was utilized in conjunction with multivariate analysis of experimental data obtained from chip-based digital polymerase chain reaction (c-dPCR), proton-nuclear magnetic resonance (^{1}H-NMR) and high-performance liquid chromatography-ultraviolet (HPLC-UV). The aim was to examine the impact of

105 introducing probiotic strains on the general metabolic activity and the kynurenine pathway activity of
106 a simplified community consisting of three intestinal isolates, which represent the small intestinal
107 microbiota.
108
109 **Material and methods**
110 *Bacteria and growth media*
111 Bacteria were selected based on their abundance in the upper small intestine, ability to metabolically
112 affect the kynurenine pathway or probiotic activity in the small intestine. *Escherichia coli* DSM11250
113 was obtained from the German collection of microorganisms and cell cultures; *Pseudomonas*
114 *fluorescens* MFY63 was obtained from the laboratory of microbiology signals and microenvironment
115 [36]; *Streptococcus salivarius* HSISS4 was obtained from the laboratory of host-microbe interactomics
116 [37]; *Streptococcus thermophilus* W69 and *Lactobacillus casei* W56 were obtained from Winclove
117 probiotics. All individual bacterial and community growth experiments were performed using
118 enriched beef broth (EBB) [38].
119
120 *Bacterial kynurenine pathway metabolism*
121 To investigate kynurenine pathway metabolism by the bacterial strains, 3 mL EBB was inoculated
122 from a glycerol stock stored at -80 °C and grown overnight at 37 °C. *E. coli* and *P. fluorescens* were
123 grown shaking at 220 RPM, *S. salivarius*, *S. thermophilus* and *L. casei* were grown without shaking.
124 Overnight grown pre-culture were diluted 1:100 in fresh EBB supplemented with 500 µM tryptophan
125 and kynurenine or kynurenic acid. At the start (0h) and at termination of the experiment (24h) 250 µL
126 culture was transferred to a new tube and immediately 1 mL cold (-20 °C) methanol was added. The
127 samples were stored at -20 °C until further use.
128
129 *Growth experiments, community construction and sampling in a mini-bioreactor*

130 All experiments were conducted in a MiniBio 250 mL bioreactor
131 (Applikon Biotechnology, The Netherlands) with a working volume of 250 mL. Each experiment was
132 performed in 200 mL EBB + 500 µM tryptophan and, if indicated 100 µM kynurenine. To prevent
133 foam accumulation 0.1 % (v/v) silicon antifoam emulsion (Carl Roth, Germany) was added. The
134 temperature, dissolved oxygen and pH were monitored online. The adaptive my-Control system
135 (Applikon Biotechnology, The Netherlands) was used to control process parameters. Setpoints of 50%
136 of the atmospheric oxygen and 37 °C were applied for dissolved oxygen and the temperature,
137 respectively [39, 40]. The culture was continuously stirred which was controlled with the adaptive
138 my-Control system. The stirrer speed increased linearly with decreasing oxygen below the setpoint
139 up to a maximum of 1200 RPM. The stirrer speed decreased linearly with increasing oxygen above
140 the setpoint down to a minimum of 220 RPM.
141 To determine kynurenine pathway metabolism of the individually grown bacteria in the bioreactor, a
142 single colony of *P. fluorescens* or 1 mL overnight grown precultures of *E. coli*, *S. salivarius*, *S.*
143 *thermophilus* or *L. casei* was added to 200 mL EBB supplemented with 500 µM tryptophan and, if
144 indicated, 100 µM kynurenine. At the start (0h) and at termination of the experiment (24h) 250 µL
145 culture was transferred to a new tube and immediately 1 mL cold (-20 °C) methanol was added. The
146 samples were stored at -20 °C until further use.
147 Community growth was obtained via inoculation of a single colony of *P. fluorescens* MFY63 in 200 mL
148 EBB supplemented with 500 µM tryptophan and, if indicated, 100 µM kynurenine. After 23 hours of
149 growth, 1 mL of combined overnight grown pre-cultures of *E. coli* (1:10000), *S. Salivarius* (1:100) and
150 *L. casei* (1:100) or *S. thermophilus* (1:100) were added. At 0, 3, 5, 7, and 24 hours after inoculation
151 with the overnight grown pre-cultures a 5 mL sample was obtained. Immediately 250 µL was added
152 to 400 µL NMR buffer (200 mM Na_2HPO_4, 44 mM NaH_2PO_4, 1 mM TSP, 3 mM NaN_3 and 20% (v/v)
153 D_2O), centrifuged at 4 °C, 21130 rcf for 20 min and 550 µL was transferred to a 5 mm NMR tube. For
154 biomass determination, 1.5 mL sample was centrifuged at room temperature for 1 min at 21130 rcf.
155 The supernatant was removed and the wet pellet was weighed. Lastly, 250 µL sample was

156 transferred to a new tube and immediately 1 mL cold (-20 °C) methanol was added. The samples
157 were stored at -20 °C until further use.
158
159 *UHPLC-UV*
160 Cell debris was removed from the sample stored at -20 °C in methanol by centrifugation at 4 °C,
161 21130 rcf for 10 min. The supernatant was transferred to a new tube and the methanol fraction was
162 evaporated using a Savant speed-vacuum dryer (SPD131, Fisher Scientific, Landsmeer, The
163 Netherlands) at 60 °C for 75 min. The dried material was reconstituted to 1 mL with 0.7% perchloric
164 acid. Samples were filtered using a 0.2 µM RC membranes (Phenomenex, Utrecht, The Netherlands)
165 and injected into the UHPLC system (Dionex UltiMate 3000 autosampler; Dionex UltiMate 3000 LPG-
166 3400SD pump, Thermo Fisher Scientific, Waltham, Massachusetts, USA). All samples were analyzed
167 on a C18 column (Kinetex 5 µm, C18 100 Å, 250 × 4.6 mm, Phenomenex, Utrecht, the Netherlands)
168 using a gradient of water/methanol with 0.1% formic acid (0 to 10 min, 95% to 80% H2O; 10 to 20
169 min, 80% to 5% H2O; 20 to 23 min, 5% H2O; 23 to 31 min, 95% H2O), with a flowrate of 1 mL/min.
170 The column was kept at a temperature of 35 °C. UV-detection at 260 nm was performed with an
171 UV6000LP Detector (Dionex Ultimate 3000 variable wavelength detector, Thermo Fisher Scientific,
172 Waltham, Massachusetts, USA) Data recording and analysis were performed using Chromeleon
173 software (version 6.8 SR13).
174
175 *DNA extraction*
176 DNA extraction was performed as previously described [41] from the cell pellets obtained by
177 centrifuging 1.5 mL culture for 1 min at 21130 rcf. The supernatant was removed, the pellets were
178 resuspended in 750 mL lysis buffer (500 mM NaCl, 50 mM Tris-HCl (pH 8.0), 50 mM EDTA, 4 % SDS)
179 and transferred to a 2 mL screw cap tube containing 0.5 g, 0.1 mm zirconia beads and 4, 3 mm glass
180 beads. The cells were disrupted with a mini-bead beater (3X 1 min, with 1 min intervals on ice) and
181 incubated at 95 °C for 15 min. Cell debris was removed by centrifugation at 4 °C, 21130 rcf for 20

182 min. 500 µL of the supernatant was transferred to a clean tube. 200 µL 10 M ammonium acetate was
183 added, and the samples were incubated for 10 min on ice. The samples were centrifuged at 4 °C,
184 21130 rcf for 10 min. 600 µL was transferred to a clean tube and 600 µL isopropanol was added. The
185 samples were incubated overnight at -20 °C and afterwards centrifuged at 4 °C, 21130 rcf for 15 min
186 to pellet the nucleic acids. The supernatant was removed and to wash the nucleic acid pellet 700 µL
187 70 % ethanol was added, the samples were mixed thoroughly and centrifuged at room temperature,
188 21130 rcf for 5 min. The pellets were completely dried by leaving the tubes open for 60 min at room
189 temperature and were dissolved in 100 µL MilliQ.
190
191 *Digital chip-based PCR analysis*
192 Chip-based digital polymerase chain reaction (c-dPCR) was performed with the QuantStudio™ 3D
193 Digital PCR System (User Guide, Catalog Number A29154, Thermo Scientific). Each c-dPCR reaction
194 was prepared in a final volume of 15,5 µL containing 5 µL QuantStudio™ 3D Digital PCR Master Mix
195 v2 (Applied Biosystems), 1 µM end concentration forward and reverse primer, 0,25 µM end
196 concentration probe **(Supplementary table 1, Eurogentec)** and nuclease free water. 1 µL extracted
197 genomic DNA was added to the reaction mix. The DNA concentration was estimated by using the
198 cycle threshold values from the qPCR run. For no-template control 1 µL nuclease free water was
199 added instead of genomic DNA. The positive control was extracted genomic DNA from pure cultures.
200 14,5 µL was loaded into the QuantStudio™ 3D Digital 20K Chip v2 using the QuantStudio™ 3D Digital
201 PCR Chip Loader. The amplification reactions were performed in the QuantStudio™ 3D Digital PCR
202 System. The PCR conditions were: 10 minutes at 96 °C for DNA polymerase activation, followed by 40
203 two-step cycles of 2 minutes at 60 °C, 30 seconds at 98 °C and a final extension for 2 minutes at 60 °C
204 and an infinite 10°C hold until the chips were read. After DNA amplification the chips were
205 transferred to the QuantStudio™ 3D Digital PCR Chip reader for imaging. The end-point fluorescence
206 data were collected and analyzed using the QuantStudio™ 3D AnalysisSuite cloud software (version
207 3.1.6-PRC-build18). Droplets were considered positive when the fluorescence signal was above the

208 threshold. The threshold was set to the positive control DNA and no-template control. The number
209 of positive and negative reactions were counted and using Poisson statistics to measure absolute
210 copies per µL.
211
212 *^{1}H NMR spectroscopy and data processing*
213 All ^{1}H-NMR spectra were recorded using a Bruker 600 MHz AVANCE II spectrometer equipped with a
214 5 mm triple resonance inverse cryoprobe and a z-gradient system. The temperature of the samples
215 was maintained at 25 °C during measurement. Prior to data acquisition, tuning and matching of the
216 probe head followed by shimming and proton pulse calibration were performed automatically for
217 each sample. One-dimensional (1D) ^{1}H-NMR spectra were recorded using the first increment of a
218 NOESY pulse sequence with presaturation (γB_1 = 50 Hz) for water suppression during a relaxation
219 delay of 4 s and a mixing time of 10 ms. 256 scans of 65,536 points covering 13,658 Hz were recorded
220 and zero filled to 65,536 complex points prior to Fourier transformation, an exponential window
221 function was applied with a line-broadening factor of 1.0 Hz. The spectra were phase and baseline
222 corrected and referenced to the internal standard (TSP; δ 0.0 ppm), using the MestReNova software
223 (v.12.0.0-20080, Mesterlab Research). With the same software, spectral alignment was performed
224 selecting manually areas and applying a linear filling method of the missing values, after the
225 exclusion of the water signal and the surrounding empty area (4.50-5.30 ppm). Spectral binning
226 followed from -0.50 to 9.00 ppm with an equal size binning step of 0.005 ppm. Noise removal was
227 performed by averaging each integrated bin separately and removing the bins with an average below
228 100. Before ordination analysis bins belonging to TSP (-0.50 – 0.72 ppm), ethanol (1.170 – 1.220 ppm
229 and 3.640 – 3.690 ppm) and a pH sensitive area (7.850 – 8.190 ppm) were removed. The annotation
230 of the bins was performed with the Chenomx Profiler software (Chenomx NMR Suite 8.6 and
231 Chenomx 600 MHz, version 11) and the HMDB database 5.0 (http://www.hmdb.ca).
232
233 *Statistical and network analysis*

234 All analysis of variance (ANOVA) were performed using GraphPad Prism 7.0. When a comparison
235 resulted in a statistically significant difference ($P < 0.05$), multiple comparisons testing was
236 performed by controlling the false discovery rate (FDR) according to the Benjamini-Hochberg method
237 ($\alpha < 0.05$). The R package MixOmics was used for ordination and multivariate statistical analysis of
238 the ^{1}H-NMR spectra [42]. The dynamic profile comparison using Kendall's τ correlation with the BH (α
239 < 0.05) was performed using the R package psych. In CytoScape 3.9.1 the plugin CoNet [43] was used
240 for network construction. The network properties were obtained using the network analyzer tool. To
241 analyze the PLS-DA separation, the accuracy, R2, Q2 and *P*-value of a permutation test performed
242 with the separation distance statistic and 1000 permutations are calculated using MetaboAnalyst 5.0
243 [44].
244
245 **Results**
246 *Kynurenine pathway metabolism and pH changes in a three species synthetic community*
247 To investigate the metabolic network changes resulting from probiotic supplementation, it is critical
248 to carefully select bacterial members for the community. These members should be isolated from
249 the normal small intestinal microbiota and capable of metabolizing key proximal small intestinal
250 metabolites such as, acetate and lactate [7]. Additionally, the kynurenine pathway should be affected
251 by the community. In this study, *Streptococcus salivarius* and two bacteria capable of affecting the
252 kynurenine pathway, namely *Pseudomonas fluorescens* and *Escherichia coli* [33, 45–47], were
253 selected. Two commonly used probiotic species, which were previously shown to be active in the
254 small intestine, *Streptococcus thermophilus* W69 [48, 49] and *Lactobacillus casei* W56 [50], were
255 added separately to distinguish between general and strain-specific effects of probiotic
256 supplementation. Before constructing the community, each species was separately grown in flasks
257 with 500 µM tryptophan and kynurenine or KYNA to investigate the ability of the various community
258 strains to metabolize kynurenine pathway metabolites. After 24 hours of incubation, kynurenine
259 pathway metabolism was observed for *P. fluorescens* and *E. coli*, but not for *S. salivarius*, *S.*

260 *thermophilus* and *L. casei* **(Supplementary figure 1)**. To confirm the kynurenine pathway metabolism
261 in conditions resembling the upper small intestine, each strain is separately grown in a
262 MiniBio 250 mL bioreactor (Applikon Biotechnology, The Netherlands) at 37 °C with controlled pO2
263 (50% of the atmospheric air) as previously described [39, 40] with and without 100 µM kynurenine.
264 After 24 hours of incubation, the results revealed that *E. coli* effectively metabolized tryptophan and
265 converted kynurenine into KYNA. Conversely, *P. fluorescens* produced only a small amount of
266 kynurenine from tryptophan. In contrast, *S. salivarius*, *S. thermophilus*, and *L. casei* did not
267 metabolize either tryptophan or kynurenine **(Supplementary figure 2A)**. These findings confirm the
268 differential metabolic capabilities of bacterial strains in relation to kynurenine pathway metabolism.
269 Concurrently, the pH dynamics of each strain cultured in the presence or absence of kynurenine were
270 assessed. *P. fluorescens* did not exhibit any noticeably pH changes during the course of the
271 experiment, whereas *E. coli*, *S. salivarius* and *S. thermophilus* demonstrated a decrease in pH after
272 3.5h of growth. *L. casei* reduced the pH after 12h of growth. Among all bacteria, only *E. coli*
273 displayed an increase in pH after 6h. Comparable pH profiles were observed for all bacteria, except
274 for *E. coli* when incubated with 100 µM kynurenine. Co-culturing *E. coli* with kynurenine resulted in
275 an earlier and more pronounced decline in pH **(Supplementary figure 2B)**.
276 The synthetic community was then grown in the bioreactor under the same conditions stated above.
277 *P. fluorescens* was initially cultured in the bioreactor for a period of 23h. Thereafter, *S. salivarius*, *E.*
278 *coli* and one of the probiotic species were added to the bioreactor to create a bacterial community.
279 Furthermore, we supplemented each community with 100 µM kynurenine to simulate increased
280 activity of the small intestinal kynurenine pathway. The small intestine is known to undergo rapid
281 changes in response to food ingestion, necessitating the need for the bacterial community to adapt
282 [16, 51]. Moreover, substantial metabolism was observed in individually grown bacteria after 3.5h of
283 growth, as indicated by the pH profile **(Supplementary figure 2B).** Therefore, we collected samples
284 from the community at 0, 3, 5, 7 and 24h after community growth and analyzed the biomass,
285 absolute species distribution using c-dPCR, metabolic environment using ^{1}H-NMR, and kynurenine

286 metabolism using HPLC-UV **(Figure 1A)**. Our results showed that both kynurenine (between 3 and 7h)
287 and KYNA (between 7 and 24h) were produced in the control and probiotic-supplemented
288 communities, with kynurenine addition increasing KYNA production in all communities
289 **(Supplementary figure 3)**. However, we observed that the addition of kynurenine together with *L.*
290 *casei* increased the production of kynurenine after 5 and 7h of growth, subsequently leading to
291 increased production of KYNA after 7 and 24h of growth compared to the control and *S.*
292 *thermophilus* supplemented communities **(Supplementary figure 3, figure 1B)**. Moreover, the pH
293 levels declined sharply after 3h of community growth, followed by a linear increase and a plateau
294 after 10h of growth **(Figure 1C)**, and the addition of kynurenine did not affect the lowest pH and the
295 time it was reached (ordinary two-way ANOVA; $F(1,12) = 1.78$, $P = 0.21$ and $F(1,12) = 0.76$, $P = 0.4$
296 respectively) **(Table 1)**. However, probiotic supplementation altered both the lowest pH and the time
297 it was reached (ordinary two-way ANOVA; $F(2,12) = 6.85$, $P = 0.01$ and $F(2,12) = 4.0$, $P = 0.047$)
298 **(Table 1)**, mostly attributed to differences between *L. casei* and *S. thermophilus* supplementation
299 **(Figure 1C, Supplementary figure 4)**, indicating a probiotic specific effect.
300 Overall, the addition of kynurenine together with *L. casei* increased the production of kynurenine and
301 subsequently KYNA compared to the control and *S. thermophilus* supplemented communities.
302 Probiotic supplementation altered both the lowest pH and the time it was reached, mostly attributed
303 to differences between *L. casei* and *S. thermophilus* supplementation, indicating a probiotic-specific
304 effect. These findings suggest that probiotics, particularly *L. casei*, may influence the production of
305 kynurenine pathway metabolites in the small intestine, which could have important implications for
306 human health.
307
308 *Effect of kynurenine and probiotic supplementation on biomass and cell counts in a simplified*
309 *bacterial community*
310 Bacteria can gain advantages in a community through utilizing the energy produced by converting
311 compounds present in the environment, inhibiting the growth of competitors, or stimulating other

312 bacteria to secrete beneficial metabolites, thereby affecting the structure and composition of the
313 community [52]. Therefore, we hypothesized that the supplementation of a probiotic species or
314 kynurenine, which was only metabolized by *P. fluorescens* and *E. coli* **(Supplementary figure 2A)**,
315 may alter the composition of the simplified community. The total biomass and the community
316 composition were compared **(Figure 1A)** to investigate the effects of kynurenine and probiotic
317 supplementation on community growth. Kynurenine addition did not affect the biomass, while
318 probiotic addition altered total biomass production after 7h of growth **(Supplementary data 1).**
319 Specifically, the addition of *L. casei* resulted in an increase in biomass in the absence of kynurenine,
320 while the introduction of *S. thermophilus* in the presence of kynurenine led to a reduction in the total
321 biomass **(Supplementary figure 5)**.
322 Next, the total cell count and cell count of specific species in the community were monitored using c-
323 dPCR. Kynurenine supplementation did not affect the total cell count or the cell count of any
324 individual species **(Supplementary data 2).** Furthermore, probiotic supplementation did not alter the
325 cell count of *P. fluorescens* **(Figure 2, Supplementary data 2)**, but probiotic supplementation altered
326 the total cell count and the cell count of *E. coli* (after 3 and 5h of growth, although multiple
327 comparison testing did not identify specific alterations), and of *S. salivarius* (after 5 and 7h of growth)
328 **(Figure 2, supplementary data 2)**, which coincides with the decrease in pH **(Figure 1C)** and with the
329 growth of *S. thermophilus* **(Figure 2).** In contrast, the cell counts of *L. casei* continuously increased
330 over time **(Figure 2)**. Cell counts of the probiotic species were not affected by kynurenine
331 supplementation at any sampling point **(Figure 2)**. Specifically, *L. casei* addition inhibited the growth
332 of *S. salivarius* by altering the community metabolism. These results suggest that the
333 supplementation of certain compounds, exemplified here by kynurenine, or probiotics, or a
334 combination of both, can alter the growth and composition of bacterial communities, which could
335 have implications for the design of probiotic therapies.
336

337 *Metabolic network analysis of probiotic supplementation and kynurenine metabolism in the synthetic*
338 *bacterial community.*
339 In order to elucidate the metabolic changes that are associated with alterations in pH, kynurenine
340 metabolism and cell count, we employed ^{1}H-NMR to analyze the supernatant **(Figure 1A).** Following
341 spectral binning and processing, a total of 943 bins were subjected to principal component analysis
342 (PCA). Our results revealed time-dependent clustering of the samples **(Figure 3A)**, whereby the most
343 significant contributors to the observed separation were lactate (bin 366, 368 and 369), acetate (bin
344 485 and 486), glucose (bin 868) and betaine (bin 880).
345 To determine whether the dynamic metabolic profiles of the community were altered by probiotic or
346 kynurenine supplementation, we conducted partial least squares – discriminant analysis (PLS-DA)
347 with cross validation (CV) and a permutation test was performed with the 943 bins as input. Our
348 analysis revealed no significant differentiation between communities with and without kynurenine
349 supplementation, nor between control and *S. thermophilus*-supplemented communities
350 **(Supplementary figure 6A and 6B)**. However, we observed significant separation in communities
351 supplemented with *L. casei,* with lactate (bin 923), glucose (bin 851 and 853) and threonine (bin 820)
352 contributing most to the separation from the control **(Figure 3B)**. Additionally, glucose (bin 848, 851
353 and 853 – 856), glycerol (bin 815) and cadaverine (bin 707) were the major contributors to the
354 differentiation between *L. casei* and *S. thermophilus* supplemented communities **(Figure 3C)**.
355 To demonstrate the metabolic contributions responsible for the variance obtained from the entire
356 spectral dataset, the chemical library of Chenomx profiler software and the online human
357 metabolome database version 5.0 were utilized. We identified 30 metabolites, and subjected the
358 area under the curve (AUC) of a representative peak for each metabolite to ordination analysis. The
359 results of this approach were similar to the ordination analyses conducted with the bins. PCA
360 revealed temporal clustering of the samples and PLS-DA revealed significant separation of the *L. casei*
361 supplemented community from the control and *S. thermophilus* supplemented communities
362 **(Supplementary figure 7A, B and C)**. Therefore, we postulated that the AUC values of the identified

363 set of metabolites may serve as a surrogate for the full spectra dataset and could be employed for
364 subsequent analysis.
365 Given that the metabolic network of a community is highly interconnected, a substantial alteration in
366 certain metabolites can lead to multiple smaller changes in related metabolites that might not be
367 detectable by ordination analysis **(Figure 3A, B and C)**. Similarly, minor effects of kynurenine
368 supplementation on metabolism may go undetected via ordination analysis. To investigate smaller
369 metabolic changes induced by kynurenine or probiotic addition to the synthetic community, we
370 compared dynamic metabolic profiles between experiments, which revealed similarities
371 **(Supplementary figure 8)** and differences in the dynamics of saccharolytic and proteolytic
372 community metabolism **(Figure 3D, Supplementary data 3)**. Of note, we observed increased lactate
373 production in the *S. thermophilus* supplemented community, which could potentially account for the
374 observed pH variation **(Figure 1C)**.
375 To explore the coordinate behavior of metabolites and network topology features across the tested
376 conditions [53], we constructed dynamic correlation-based networks using the Cytoscape plugin
377 CoNet [43], whereby the nodes represent the metabolites and the edges represent correlations
378 between the metabolic profiles per condition. Without kynurenine, *S. thermophilus* supplementation
379 decreased the number of edges and the clustering coefficient, while the metabolite with the highest
380 number of edges was aspartate (7), compared to cadaverine (12) in the control network **(Figure 3E,**
381 **table 2)**. *L. casei* supplementation had a more drastic effect on the network, increasing the number
382 of edges, clustering coefficient and network density substantially **(Figure 3E, table 2)**. Kynurenine
383 supplementation reduced the number of edges, including indole, present in the control community
384 network, and reduced the number of edges of cadaverine from 12 to 1. Consequently, cadaverine
385 and indole no longer connected two major hubs of connected metabolites compared to control
386 community. The clustering coefficient and network density of the control community supplemented
387 with kynurenine was 1, due to the connections between all the metabolites with all the other
388 metabolites in each hub **(Figure 3E, table 2)**. Kynurenine supplementation to the *S. thermophilus* and

389 *L. casei* supplemented communities increased the number of edges, clustering coefficient and
390 network density, with indole and cadaverine being the metabolites with the most edges, similar to
391 the control network without kynurenine supplementation **(Figure 3E, table 2).** The node degree and
392 betweenness centrality of individual metabolites were also analyzed, showing probiotic-specific
393 effects on the community metabolism as well as an effect of kynurenine supplementation on
394 cadaverine metabolism **(Supplementary data 4)**. Together the network analysis revealed probiotic-
395 specific effects on the community metabolism and an effect of kynurenine supplementation on
396 clustering coefficient, network density and node parameters of the metabolic networks, mainly due
397 to alterations in cadaverine utilization.

398 **Discussion**

399 The present study investigated the impact of probiotic supplementation on metabolism of the small
400 intestinal microbiota. To achieve this, we constructed a synthetic community consisting of three gut
401 isolates that mimicked the microbial community of the upper small intestine. Specifically, we
402 examined the metabolic impact of probiotic supplementation on both general metabolism and the
403 kynurenine pathway, which has been implicated in the modulation of immune responses and
404 neuroinflammation. Our findings shed light on the probiotic-specific mechanisms of action that drive
405 colonization resistance in the small intestine and suggest that the kynurenine pathway may be a
406 promising target for future probiotic-based therapies aimed at promoting intestinal health.

407 Probiotics are known to exert their effects through competitive exclusion often by reducing the pH of
408 the gut milieu through increased lactate production [54]. In our study, supplementation with *S.*
409 *thermophilus* led to increased lactate production, resulting in a reduction in pH, and accompanied by
410 a decrease in formate and acetate levels **(Figure 3D and 1C)**. However, this supplementation did not
411 result in significant changes to the composition of the community **(Figure 2)** or the dynamic
412 metabolic network **(Figure 3E)**. Conversely, when *L. casei* was supplemented, we observed a
413 reduction in the growth of *S. salivarius*, which was not accompanied by increased lactate production
414 **(Figure 2, 3D)**. Other studies have also reported beneficial effects of *L. casei* supplementation

415 independent of acidification or lactate production [55]. These results suggest that *L. casei*
416 supplementation alters the metabolic environment, enhancing the resistance of the community to
417 perturbations and improving metabolic utilization **(Figure 3D and E).** This finding is consistent with
418 previous studies showing a positive association between habitual *L. casei* Shirota intake and long-
419 term compositional stability of the fecal microbiota [56].
420 The concept of direct colonization resistance refers to the ability of the resident microbiota to resist
421 the colonization and expansion of invading species [57]. However, decreased diversity can lead to
422 unoccupied ecological niches that can be occupied by invading species potentially harmful to host
423 health [58]. Probiotics have been proposed as a means to increase colonization resistance by filling
424 unoccupied niches before pathogenic species can colonize [59]. However, current probiotic
425 interventions do not take into account the functional capacity of probiotics to occupy specific niches
426 in the gut [60], which may explain the variable effectiveness of probiotics [61]. To address this,
427 synthetic communities are constructed [22, 62–65], but the lack of molecular insights has hampered
428 the development of probiotic therapies. The genetic capacity of *L. casei* in our synthetic community
429 of three species made it more functionally diverse **(Figure 3D)** compared to the three initial
430 community members compared to *S. thermophilus*, which resembles *S. salivarius*. Thus, *L. casei*
431 increased the resistance to perturbations and metabolic utilization **(Figure 3E, table 3),** by occupying
432 an empty ecological niche, whereas *S. thermophilus* had to compete for the ecological niche
433 occupied by *S. salivarius*. However, the ability to occupy a niche is determined by the functional
434 capability [66] and the environment [67]. Therefore, selecting strains with a wide range of functional
435 capacities and constructing a diverse multispecies probiotic formula could be a promising approach
436 for developing effective probiotic therapies [18, 68]
437 Indirect colonization resistance involves improving the gut epithelial barrier or enhancing the hosts
438 immune system [69]. Metabolites produced by the microbiota can interact with the host and
439 improve gut integrity. For example, stimulation of GPR35 by KYNA, was shown to enhance mucosal
440 repair and stimulate mucus secretion, which increases the integrity of the gut epithelial barrier [70,

441 71]. Thus, increasing microbial production of KYNA in the small intestine may indirectly increase
442 colonization resistance. Although no in vivo studies were conducted in our study to confirm
443 improved intestinal barrier integrity due to increased microbial KYNA production resulting from
444 probiotic addition, we show that in the *L. casei* supplemented community, *E. coli* had a reduced
445 impact on the metabolic environment since the node degree and betweenness centrality of the *E.*
446 *coli* produced metabolites cadaverine [72] and indole [73] were lower **(Figure 3E)**. In *kynurenine*
447 *and S. thermophilus supplemented community, E. coli* had an increased impact on the metabolic
448 environment **(Supplementary figure 1 and 2),** even though this effect was not translated into
449 increased cell counts for *E. coli* **(Figure 2)**.
450 Overall, the present study demonstrates that supplementation with different probiotics can lead to
451 distinct alterations in the metabolic environment of the microbiota community, with *L. casei*
452 enhancing resistance to perturbations and improving metabolic utilization. Our findings suggest that
453 selecting probiotic strains with a wide range of genetic capabilities, which complement the functional
454 capacity of the residing microbiota or constructing a diverse multispecies formula may be a
455 promising approach for developing effective probiotic therapies. Additionally, the present findings
456 suggest that increasing microbial production of metabolites such as KYNA in the small intestine may
457 indirectly improve intestinal barrier integrity and increase colonization resistance. Further in vivo
458 studies are necessary to confirm the effects of probiotic supplementation on intestinal barrier
459 integrity and to develop probiotic therapies that target specific ecological niches in the gut.
460
461 **Author Contributions:** JJ, SEA: Conceptualization, investigation, writing-original draft, and editing; JJ,
462 ACC, KC: data analysis; JJ, ACC: methodology; SvH: Conceptualization, writing review; SEA: funding
463 acquisition. All authors have read and agreed to the published version of the manuscript.
464 **Acknowledgements:** We thank Valeria Mathlener of Winclove, B.V. assisting us with the c-dPCR
465 measurements.

466 **Conflicts of Interest:** S. van Hemert is employee in Winclove (Winclove manufactures and markets
467 probiotics). The content of this study was neither influenced nor constrained by this fact. The other
468 authors have no conflicts of interest to declare.

469 **Funding:** SEA has received research funding support from Winclove, B.V. This support neither
470 influenced nor constrained the contents of this article

471 **Data availability:** The raw ^{1}H-NMR data was deposited in the Metabolights public repository [74]
472 under the accession number: MTBLS7370

473 **Tables**

474 **Table 1: properties of the pH profile of each community**.
475 The mean ± SD of the lowest pH value and time the lowest pH value was reached for all communities
476 with and without kynurenine (kyn) supplementation.

Communities	Lowest pH value	Time of the lowest pH value (h)
Control	5.69 ± 0.09	4.7 ± 0.2
S. thermophilus	5.56 ± 0.08	3.8 ± 0.1
L. casei	5.77 ± 0.03	4.5 ± 0.7
Control + kyn	5.77 ± 0.17	4.0 ± 0.2
***S. thermophilus* + kyn**	5.53 ± 0.11	3.9 ± 0.3
***L. casei* + kyn**	6.05 ± 0.25	4.6 ± 0.4

477

478

479 **Table 2: Properties of the dynamic correlation-based metabolic networks for each community**. The
480 number of nodes, edges, clustering coefficient, network density and the nodes with the most edges
481 of the networks depicted in figure 3E for the communities with probiotic or kynurenine (kyn)
482 supplementation.

Communities	Nodes	Edges	Clustering coefficient	Network density	Node with the most edges (edges)
Control	24	54	0.857	0.368	Cadaverine (12)
S. thermophilus	23	40	0.794	0.374	Aspartate (7)
L. casei	17	94	0.935	0.886	Gluconolactone/gluconate, glycerol (14)
***L. casei* + kyn**	24	103	0.892	0.654	Glucose, tryptophan, glycerol (16)
***S. thermophilus* + kyn**	20	56	0.901	0.549	Indole, cadaverine (12)
Control + kyn	20	54	1	1	Tryptophan, phenylalanine, alanine, methionine, glutamate, proline, isoleucine, glycine, valine, tyrosine (9)

483 **Figure legends**

484 **Figure 1: *Lactobacillus casei* supplementation increases kynurenine pathway metabolism in a**
485 **synthetic community**

486 A) Overview of the construction of the community and sampling procedure. *P. fluorescens* was
487 inoculated 23h prior to inoculating other species with probiotics. PH and pO_2 (indicated with dashed
488 line) were continuously measured. Black arrows indicate sampling points (0, 3, 5, 7 and 24h) for
489 obtaining metabolomics, compositional and biomass data. All experiments were performed in
490 triplicates. B) Boxplots showing the area under the curve (AUC) for kynurenine and kynurenic acid as
491 measured from the HPLC-UV chromatograms normalized to the AUC of the initial tryptophan peak
492 obtained from -23h. Significant comparisons are depicted with letters (a-d): a: $q < 0.05$, b: $q < 0.01$, c:
493 $q < 0.001$ and d: $q < 0.0001$ as obtained with an ordinary two-way ANOVA and multiple comparisons
494 testing by controlling the false discovery rate according to the Benjamini-Hochberg procedure. C) pH
495 profile for control, *S. thermophilus* supplemented and *L. casei* supplemented communities
496 with/without kynurenine. Sampling points indicated by dashed lines. Boxplot indicates the lowest pH
497 value per condition. Significant differences are indicated with asterisks; *, $q < 0.05$, as obtained with
498 an ordinary one-way ANOVA and multiple comparison testing by controlling the false discovery rate
499 according to the Benjamini-Hochberg procedure.

500

501 **Figure 2: Supplementation of *Lactobacillus casei* reduces the growth of *Streptococcus salivarius* in a**
502 **simplified community**

503 Boxplots of total cell count and cell count per species of a simplified community (*E. coli*, *S. salivarius*
504 and *P. fluorescens*) determined after 3, 5, 7 and 24h of growth. Cell counts of the communities grown
505 with the supplemented probiotic species *L. casei* or *S. thermophilus* are depicted in different colors.
506 Control or probiotic supplemented communities grown with 100 µM kynurenine are shown with
507 stripes. Statistical differences between communities were determined by ordinary two way ANOVA
508 approach per timepoint, and significant differences ($q < 0.05$) after multiple comparisons testing by

509 controlling the false discovery rate according to the Benjamini-Hochberg procedure are indicated
510 with asterisks. Probiotic addition altered the cell count of *E. coli* after 3 and 5h of growth, and the cell
511 count of *S. salivarius* after 7h of growth (ordinary two-way ANOVA: $F(2,12) = 4.43$ and $P = 0.036$,
512 $F(2,12) = 4.15$, $P = 0.043$ and $F(2,12) = 7.62$, $P = 0.007$ respectively), but multiple comparisons testing
513 did not yield any significant differences. Cell counts of added probiotic species grown with and
514 without kynurenine per timepoint were compared by performing an unpaired t test.

515 **Figure 3: Probiotic and kynurenine supplementation alter the metabolism of a simplified**
516 **community in a specific manner**

517 A) PCA with binned ^{1}H-NMR spectra as input showing separation of metabolites with lactate (bin
518 366,368 and 369), acetate (bin 485 and 486), glucose (bin 868), and betaine (bin 880) being the most
519 distinguishing factors (indicated with arrows). The ellipses represent the 95 % confidence interval. B)
520 PLS-DA with binned ^{1}H-NMR spectra of control and *L. casei* supplemented communities, indicating
521 lactate (bin 923), glucose (bin 851 and 853), and threonine (bin 820) as contributing factors. C) PLS-
522 DA with binned ^{1}H-NMR spectra of *S. thermophilus* and *L. casei* supplemented communities
523 indicating glucose (bin 848, 851 and 853 – 856), glycerol, (bin 815) and cadaverine (bin 707) as
524 contributing factors. Statistical parameter accuracy, R2 and Q2 and *P*-values are included. The *P*-
525 value is the results of a permutation test performed with the separation distance statistic and 1000
526 permutations. All parameters were calculated using MetaboAnalyst 5.0. D) Dynamic profiles of the
527 significantly different saccharolytic and proteolytic metabolites with repeated measure two-way
528 ANOVA showing significant differences. The error bars indicate the standard deviation. The
529 timepoints where a significant result of multiple comparison testing by controlling the false discovery
530 rate according to the Benjamini-Hochberg procedure is obtained are indicated with an asterisk; *: $q <$
531 0.05, detailed results of the multiple comparison tests can be found in the supplementary data 3. E)
532 Dynamic correlation-based networks of all measured metabolites in the communities showing
533 positive and negative correlations via red solid and blue dashed edges, respectively. Nodes represent
534 metabolites. Edges represents correlations between the two connected nodes, obtained when 2/3

535 methods give a positive results; Kendall's -0.9 > τ > 0.9, Spearman's -0.9 > ρ > 0.9. Brown's
536 randomization method with 1000 iterations had a Benjamini-Hochberg corrected *P*-value < 0.05. The
537 calculation of the edges was performed using the Cytoscape plugin CoNet.

538

539

540

541 **References**

542 1. Hou K, Wu ZX, Chen XY, Wang JQ, Zhang D, Xiao C, et al. Microbiota in health and
543 diseases. *Signal Transduction and Targeted Therapy 2022 7:1* 2022; **7**: 1–28.
544 2. de Vos WM, Tilg H, van Hul M, Cani PD. Gut microbiome and health: mechanistic
545 insights. *Gut* 2022; **71**: 1020–1032.
546 3. Donaldson GP, Lee SM, Mazmanian SK. Gut biogeography of the bacterial microbiota.
547 *Nat Rev Microbiol* 2016; **14**: 20.
548 4. Leite G, Morales W, Weitsman S, Celly S, Parodi G, Mathur R, et al. The duodenal
549 microbiome is altered in small intestinal bacterial overgrowth. *PLoS One* 2020; **15**:
550 e0234906.
551 5. Villmones HC, Svanevik M, Ulvestad E, Stenstad T, Anthonisen IL, Nygaard RM, et al.
552 Investigating the human jejunal microbiota. *Sci Rep* 2022; **12**.
553 6. Roberti MP, Rauber C, Kroemer G, Zitvogel L. Impact of the ileal microbiota on colon
554 cancer. *Semin Cancer Biol* 2022; **86**: 955–966.
555 7. Zoetendal EG, Raes J, van den Bogert B, Arumugam M, Booijink CC, Troost FJ, et al.
556 The human small intestinal microbiota is driven by rapid uptake and conversion of
557 simple carbohydrates. *The ISME Journal 2012 6:7* 2012; **6**: 1415–1426.
558 8. Kaczmarczyk M, Löber U, Adamek K, Węgrzyn D, Skonieczna-Żydecka K, Malinowski D,
559 et al. The gut microbiota is associated with the small intestinal paracellular
560 permeability and the development of the immune system in healthy children during
561 the first two years of life. *Journal of Translational Medicine 2021 19:1* 2021; **19**: 1–26.
562 9. Martinez-Guryn K, Hubert N, Frazier K, Urlass S, Musch MW, Ojeda P, et al. Small
563 intestine microbiota regulate host digestive and absorptive adaptive responses to
564 dietary lipids. *Cell Host Microbe* 2018; **23**: 458.
565 10. Roberti MP, Rauber C, Kroemer G, Zitvogel L. Impact of the ileal microbiota on colon
566 cancer. *Semin Cancer Biol* 2022; **86**: 955–966.
567 11. Nouvenne A, Ticinesi A, Tana C, Prati B, Catania P, Miraglia C, et al. Digestive disorders
568 and Intestinal microbiota. *Acta Bio Medica: Atenei Parmensis* 2018; **89**: 47.
569 12. Wong AC, Levy M. New Approaches to Microbiome-Based Therapies. *mSystems* 2019;
570 **4**.
571 13. Hill C, Guarner F, Reid G, Gibson GR, Merenstein DJ, Pot B, et al. The International
572 Scientific Association for Probiotics and Prebiotics consensus statement on the scope
573 and appropriate use of the term probiotic. *Nature Reviews Gastroenterology &*
574 *Hepatology 2014 11:8* 2014; **11**: 506–514.

575 14. Barbosa SJ de A, Oliveira MMB, Ribeiro SB, de Medeiros CACX, Lima ML de S, Guerra
576 GCB, et al. The beneficial effects of Lacticaseibacillus casei on the small intestine and
577 colon of Swiss mice against the deleterious effects of 5-fluorouracil. *Front Immunol*
578 2022; **13**: 6411.
579 15. Zhong C, Qu C, Wang B, Liang S, Zeng B. Probiotics for Preventing and Treating Small
580 Intestinal Bacterial Overgrowth. *J Clin Gastroenterol* 2017; **51**: 300–311.
581 16. Yilmaz B, Fuhrer T, Morgenthaler D, Krupka N, Wang D, Spari D, et al. Plasticity of the
582 adult human small intestinal stoma microbiota. *Cell Host Microbe* 2022; **30**: 1773-
583 1787.e6.
584 17. Colom J, Freitas D, Simon A, Brodkorb A, Buckley M, Deaton J, et al. Presence and
585 Germination of the Probiotic Bacillus subtilis DE111® in the Human Small Intestinal
586 Tract: A Randomized, Crossover, Double-Blind, and Placebo-Controlled Study. *Front*
587 *Microbiol* 2021; **12**: 2189.
588 18. Jansma J, Thome NU, Schwalbe M, Chatziioannou AC, Elsayed SS, Wezel GP van, et al.
589 Probiotics supplementation to adult human small intestinal stoma microbiota causes
590 dynamic increase in the community resistance to perturbations and nutrient
591 utilization. *bioRxiv* 2023; 2023.01.29.525861.
592 19. Weiss AS, Burrichter AG, Durai Raj AC, von Strempel A, Meng C, Kleigrewe K, et al. In
593 vitro interaction network of a synthetic gut bacterial community. *The ISME Journal*
594 *2021 16:4* 2021; **16**: 1095–1109.
595 20. Großkopf T, Soyer OS. Synthetic microbial communities. *Curr Opin Microbiol* 2014; **18**:
596 72–77.
597 21. Christensen BB, Haagensen JAJ, Heydorn A, Molin S. Metabolic Commensalism and
598 Competition in a Two-Species Microbial Consortium. *Appl Environ Microbiol* 2002; **68**:
599 2495.
600 22. Cheng AG, Ho PY, Aranda-Díaz A, Jain S, Yu FB, Meng X, et al. Design, construction, and
601 in vivo augmentation of a complex gut microbiome. *Cell* 2022; **185**: 3617-3636.e19.
602 23. Gutiérrez N, Garrido D. Species Deletions from Microbiome Consortia Reveal Key
603 Metabolic Interactions between Gut Microbes. *mSystems* 2019; **4**.
604 24. Kleerebezem M, Binda S, Bron PA, Gross G, Hill C, van Hylckama Vlieg JE, et al.
605 Understanding mode of action can drive the translational pipeline towards more
606 reliable health benefits for probiotics. *Curr Opin Biotechnol* 2019; **56**: 55–60.
607 25. Clark RL, Connors BM, Stevenson DM, Hromada SE, Hamilton JJ, Amador-Noguez D, et
608 al. Design of synthetic human gut microbiome assembly and butyrate production.
609 *Nature Communications 2021 12:1* 2021; **12**: 1–16.
610 26. Blasche S, Kim Y, Oliveira AP, Patil KR. Model microbial communities for ecosystems
611 biology. *Curr Opin Syst Biol* 2017; **6**: 51–57.
612 27. Tanoue T, Morita S, Plichta DR, Skelly AN, Suda W, Sugiura Y, et al. A defined
613 commensal consortium elicits CD8 T cells and anti-cancer immunity. *Nature 2019*
614 *565:7741* 2019; **565**: 600–605.
615 28. Savitz J, Savitz jsavitz J. The kynurenine pathway: a finger in every pie. *Molecular*
616 *Psychiatry 2019 25:1* 2019; **25**: 131–147.
617 29. Laurans L, Venteclef N, Haddad Y, Chajadine M, Alzaid F, Metghalchi S, et al. Genetic
618 deficiency of indoleamine 2,3-dioxygenase promotes gut microbiota-mediated
619 metabolic health. *Nature Medicine 2018 24:8* 2018; **24**: 1113–1120.
620 30. Kaya B, Melhem H, Niess JH. GPR35 in Intestinal Diseases: From Risk Gene to Function.
621 *Front Immunol* 2021; **12**: 4610.

622 31. Turski MP, Turska M, Paluszkiewicz P, Parada-Turska J, Oxenkrug GF. Kynurenic Acid in
623 the Digestive System–-New Facts, New Challenges. *International Journal of*
624 *Tryptophan Research* 2013; **6**: IJTR.S12536.
625 32. Kuc D, Zgrajka W, Parada-Turska J, Urbanik-Sypniewska T, Turski WA. Micromolar
626 concentration of kynurenic acid in rat small intestine Short Communication. *Amino*
627 *Acids* 2008; **35**: 503–505.
628 33. Kurnasov O, Goral V, Colabroy K, Gerdes S, Anantha S, Osterman A, et al. NAD
629 Biosynthesis: Identification of the Tryptophan to Quinolinate Pathway in Bacteria.
630 *Chem Biol* 2003; **10**: 1195–1204.
631 34. Więdłocha M, Marcinowicz P, Janoska-Jaździk M, Szulc A. Gut microbiota, kynurenine
632 pathway and mental disorders – Review. *Prog Neuropsychopharmacol Biol Psychiatry*
633 2021; **106**: 110145.
634 35. Purton T, Staskova L, Lane MM, Dawson SL, West M, Firth J, et al. Prebiotic and
635 probiotic supplementation and the tryptophan-kynurenine pathway: A systematic
636 review and meta analysis. *Neurosci Biobehav Rev* 2021; **123**: 1–13.
637 36. Chapalain A, Rossignol G, Lesouhaitier O, Merieau A, Gruffaz C, Guerillon J, et al.
638 Comparative study of 7 fluorescent pseudomonad clinical isolates.
639 *https://doi.org/101139/W07-110* 2007; **54**: 19–27.
640 37. van den Bogert B, Boekhorst J, Herrmann R, Smid EJ, Zoetendal EG, Kleerebezem M.
641 Comparative Genomics Analysis of Streptococcus Isolates from the Human Small
642 Intestine Reveals their Adaptation to a Highly Dynamic Ecosystem. *PLoS One* 2013; **8**:
643 e83418.
644 38. Waclawiková B, Bullock A, Schwalbe M, Aranzamendi C, Nelemans SA, van Dijk G, et
645 al. Gut bacteria-derived 5-hydroxyindole is a potent stimulant of intestinal motility via
646 its action on L-type calcium channels. *PLoS Biol* 2021; **19**: e3001070.
647 39. He G, Shankar RA, Chzhan M, Samouilov A, Kuppusamy P, Zweier JL. Noninvasive
648 measurement of anatomic structure and intraluminal oxygenation in the
649 gastrointestinal tract of living mice with spatial and spectral EPR imaging. *Proc Natl*
650 *Acad Sci U S A* 1999; **96**: 4586.
651 40. Sheridan WG, Lowndes RH, Young HL. Intraoperative tissue oximetry in the human
652 gastrointestinal tract. *The American Journal of Surgery* 1990; **159**: 314–319.
653 41. Yu Z, Morrison M. Improved extraction of PCR-quality community DNA from digesta
654 and fecal samples. *Biotechniques* 2004; **36**: 808–812.
655 42. Rohart F, Gautier B, Singh A, Lê Cao KA. mixOmics: An R package for 'omics feature
656 selection and multiple data integration. *PLoS Comput Biol* 2017; **13**: e1005752.
657 43. Faust K, Raes J, Wilmes P, Heintz-Buschart A, Eiler A. CoNet app: inference of
658 biological association networks using Cytoscape. *F1000Research 2016 5:1519* 2016; **5**:
659 1519.
660 44. Xia J, Psychogios N, Young N, Wishart DS. MetaboAnalyst: A web server for
661 metabolomic data analysis and interpretation. *Nucleic Acids Res* 2009; **37**.
662 45. Bortolotti P, Hennart B, Thieffry C, Jausions G, Faure E, Grandjean T, et al. Tryptophan
663 catabolism in Pseudomonas aeruginosa and potential for inter-kingdom relationship.
664 *BMC Microbiol* 2016; **16**: 1–10.
665 46. Paulsen IT, Press CM, Ravel J, Kobayashi DY, Myers GSA, Mavrodi D v., et al. Complete
666 genome sequence of the plant commensal Pseudomonas fluorescens Pf-5. *Nature*
667 *Biotechnology 2005 23:7* 2005; **23**: 873–878.

668 47. Kuc D, Zgrajka W, Parada-Turska J, Urbanik-Sypniewska T, Turski WA. Micromolar
669 concentration of kynurenic acid in rat small intestine. *Amino Acids* 2008; **35**: 503–505.
670 48. Martinović A, Cocuzzi R, Arioli S, Mora D. Streptococcus thermophilus: To Survive, or
671 Not to Survive the Gastrointestinal Tract, That Is the Question! *Nutrients* 2020; **12**: 1–
672 13.
673 49. Mater DDG, Drouault-Holowacz S, Oozeer R, Langella P, Anba J, Corthier G. β-
674 Galactosidase production by Streptococcus thermophilus is higher in the small
675 intestine than in the caecum of human-microbiota-associated mice after lactose
676 supplementation. *British Journal of Nutrition* 2006; **96**: 177–181.
677 50. Timmerman HM, Niers LEM, Ridwan BU, Koning CJM, Mulder L, Akkermans LMA, et al.
678 Design of a multispecies probiotic mixture to prevent infectious complications in
679 critically ill patients. *Clinical Nutrition* 2007; **26**: 450–459.
680 51. Procházková N, Falony G, Dragsted LO, Licht TR, Raes J, Roager HM. Advancing human
681 gut microbiota research by considering gut transit time. *Gut* 2022; **0**: gutjnl-2022-
682 328166.
683 52. Fritts RK, McCully AL, McKinlay JB. Extracellular Metabolism Sets the Table for
684 Microbial Cross-Feeding. *Microbiology and Molecular Biology Reviews* 2021; **85**.
685 53. Batushansky A, Matsuzaki S, Newhardt MF, West MS, Griffin TM, Humphries KM. GC-
686 MS metabolic profiling reveals Fructose-2,6-bisphosphate regulates branched chain
687 amino acid metabolism in the heart during fasting. *Metabolomics* 2019; **15**: 18.
688 54. van Zyl WF, Deane SM, Dicks LMT. Molecular insights into probiotic mechanisms of
689 action employed against intestinal pathogenic bacteria. *Gut Microbes* 2020; **12**.
690 55. Panpetch W, Phuengmaung P, Cheibchalard T, Somboonna N, Leelahavanichkul A,
691 Tumwasorn S. Lacticaseibacillus casei Strain T21 Attenuates Clostridioides difficile
692 Infection in a Murine Model Through Reduction of Inflammation and Gut Dysbiosis
693 With Decreased Toxin Lethality and Enhanced Mucin Production. *Front Microbiol*
694 2021; **12**: 3607.
695 56. Amamoto R, Shimamoto K, Park S, Matsumoto H, Shimizu K, Katto M, et al. Yearly
696 changes in the composition of gut microbiota in the elderly, and the effect of
697 lactobacilli intake on these changes. *Scientific Reports 2021 11:1* 2021; **11**: 1–14.
698 57. Sorbara MT, Pamer EG. Interbacterial mechanisms of colonization resistance and the
699 strategies pathogens use to overcome them. *Mucosal Immunology 2018 12:1* 2018;
700 **12**: 1–9.
701 58. Khan I, Bai Y, Zha L, Ullah N, Ullah H, Shah SRH, et al. Mechanism of the Gut
702 Microbiota Colonization Resistance and Enteric Pathogen Infection. *Front Cell Infect*
703 *Microbiol* 2021; **11**: 1273.
704 59. Litvak Y, Bäumler AJ. The founder hypothesis: A basis for microbiota resistance,
705 diversity in taxa carriage, and colonization resistance against pathogens. *PLoS Pathog*
706 2019; **15**.
707 60. Zmora N, Zilberman-Schapira G, Suez J, Mor U, Dori-Bachash M, Bashiardes S, et al.
708 Personalized Gut Mucosal Colonization Resistance to Empiric Probiotics Is Associated
709 with Unique Host and Microbiome Features. *Cell* 2018; **174**: 1388-1405.e21.
710 61. Kristensen NB, Bryrup T, Allin KH, Nielsen T, Hansen TH, Pedersen O. Alterations in
711 fecal microbiota composition by probiotic supplementation in healthy adults: A
712 systematic review of randomized controlled trials. *Genome Med* 2016; **8**: 1–11.

713 62. Pereira FC, Wasmund K, Cobankovic I, Jehmlich N, Herbold CW, Lee KS, et al. Rational
714 design of a microbial consortium of mucosal sugar utilizers reduces Clostridiodes
715 difficile colonization. *Nature Communications 2020 11:1* 2020; **11**: 1–15.
716 63. Brand MW, Wannemuehler MJ, Phillips GJ, Proctor A, Overstreet AM, Jergens AE, et
717 al. The Altered Schaedler Flora: Continued Applications of a Defined Murine Microbial
718 Community. *ILAR J* 2015; **56**: 169–178.
719 64. Darnaud M, De Vadder F, Bogeat P, Boucinha L, Bulteau AL, Bunescu A, et al. A
720 standardized gnotobiotic mouse model harboring a minimal 15-member mouse gut
721 microbiota recapitulates SOPF/SPF phenotypes. *Nature Communications 2021 12:1*
722 2021; **12**: 1–21.
723 65. Brugiroux S, Beutler M, Pfann C, Garzetti D, Ruscheweyh HJ, Ring D, et al. Genome-
724 guided design of a defined mouse microbiota that confers colonization resistance
725 against Salmonella enterica serovar Typhimurium. *Nature Microbiology 2016 2:2*
726 2016; **2**: 1–12.
727 66. Aktas B, De Wolfe TJ, Safdar N, Darien BJ, Steele JL. The Impact of Lactobacillus casei
728 on the Composition of the Cecal Microbiota and Innate Immune System Is Strain
729 Specific. *PLoS One* 2016; **11**: e0156374.
730 67. Colombo M, Oliveira AEZ de, Carvalho AF de, Nero LA. Development of an alternative
731 culture medium for the selective enumeration of Lactobacillus casei in fermented
732 milk. *Food Microbiol* 2014; **39**: 89–95.
733 68. Chapman CMC, Gibson GR, Rowland I. In vitro evaluation of single- and multi-strain
734 probiotics: Inter-species inhibition between probiotic strains, and inhibition of
735 pathogens. *Anaerobe* 2012; **18**: 405–413.
736 69. Sassone-Corsi M, Raffatellu M. No vacancy: how beneficial microbes cooperate with
737 immunity to provide colonization resistance to pathogens. *J Immunol* 2015; **194**:
738 4081–4087.
739 70. Kaya B, Melhem H, Niess JH. GPR35 in Intestinal Diseases: From Risk Gene to Function.
740 *Front Immunol* 2021; **12**: 4610.
741 71. Wang Z, Yin L, Qi Y, Zhang J, Zhu H, Tang J. Intestinal Flora-Derived Kynurenic Acid
742 Protects Against Intestinal Damage Caused by Candida albicans Infection via
743 Activation of Aryl Hydrocarbon Receptor. *Front Microbiol* 2022; **13**: 2554.
744 72. Akhova A, Nesterova L, Shumkov M, Tkachenko A. Cadaverine biosynthesis
745 contributes to decreased Escherichia coli susceptibility to antibiotics. *Res Microbiol*
746 2021; **172**: 103881.
747 73. Piñero-Fernandez S, Chimerel C, Keyser UF, Summers DK. Indole transport across
748 Escherichia coli membranes. *J Bacteriol* 2011; **193**: 1793–1798.
749 74. Haug K, Salek RM, Conesa P, Hastings J, De Matos P, Rijnbeek M, et al. MetaboLights -
750 An open-access general-purpose repository for metabolomics studies and associated
751 meta-data. *Nucleic Acids Res* 2013; **41**.
752

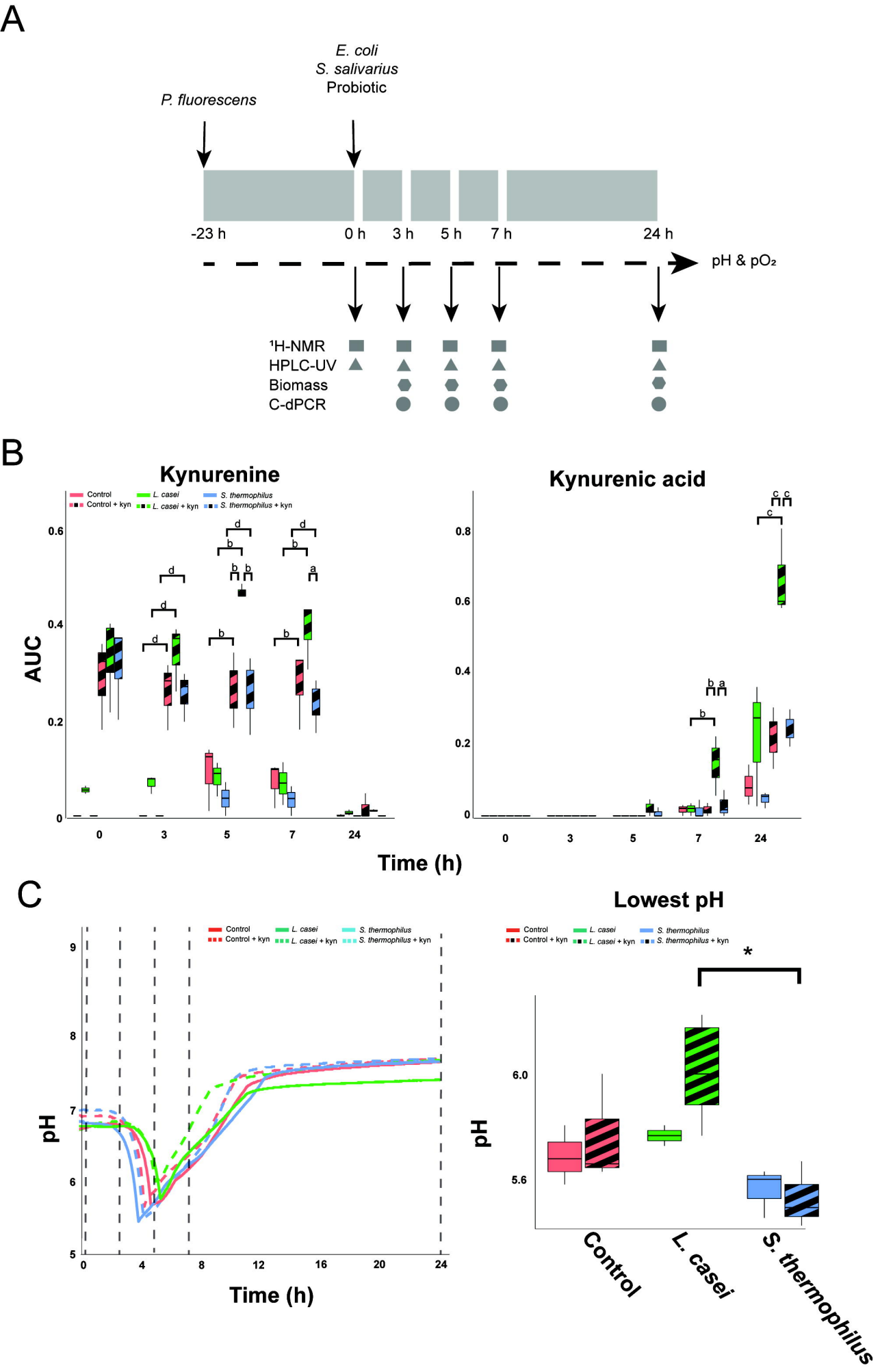
A
E. coli
S. salivarius
Probiotic
P. fluorescens
-23 h
0 h
3 h
5 h
7 h
24 h
pH & pO₂
¹H-NMR
HPLC-UV
Biomass
C-dPCR
B
Kynurenine
Kynurenic acid
Control
Control + kyn
L. casei
L. casei + kyn
S. thermophilus
S. thermophilus + kyn
AUC
Time (h)
C
pH
Time (h)
Lowest pH
Control
L. casei
S. thermophilus

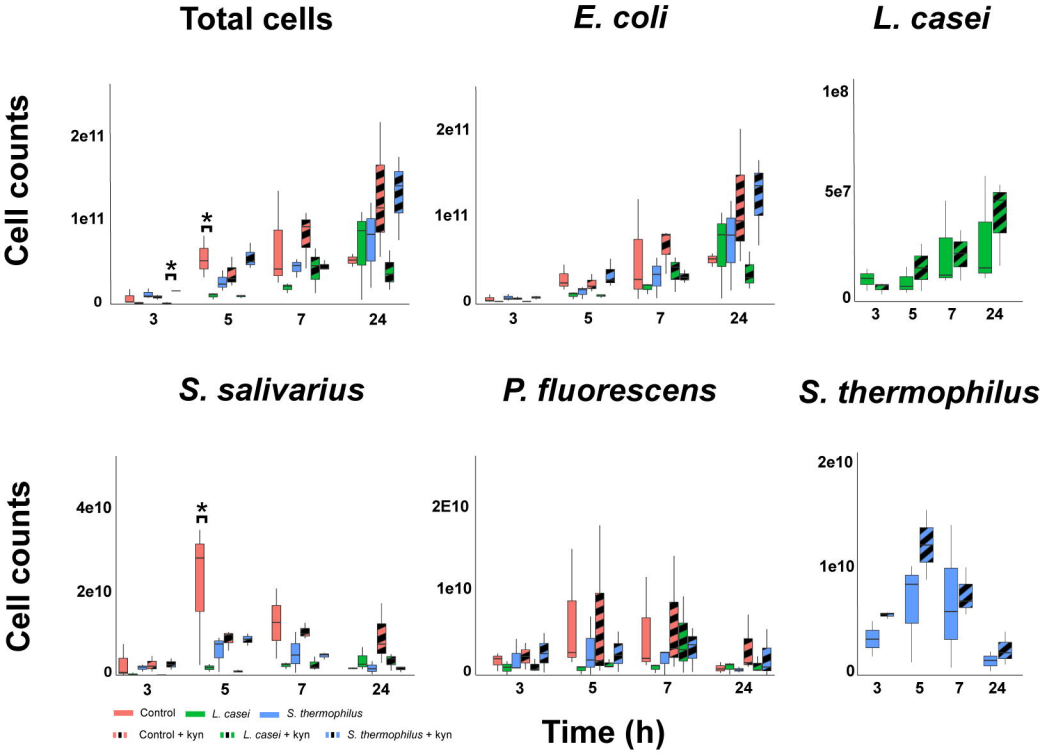
Total cells
E. coli
L. casei
S. salivarius
P. fluorescens
S. thermophilus
Cell counts
Cell counts
2e11
1e11
0
2e11
1e11
0
1e8
5e7
0
4e10
2e10
0
2E10
1e10
0
2e10
1e10
0
*
*
*
3
5
7
24
Control
L. casei
S. thermophilus
Control + kyn
L. casei + kyn
S. thermophilus + kyn
Time (h)

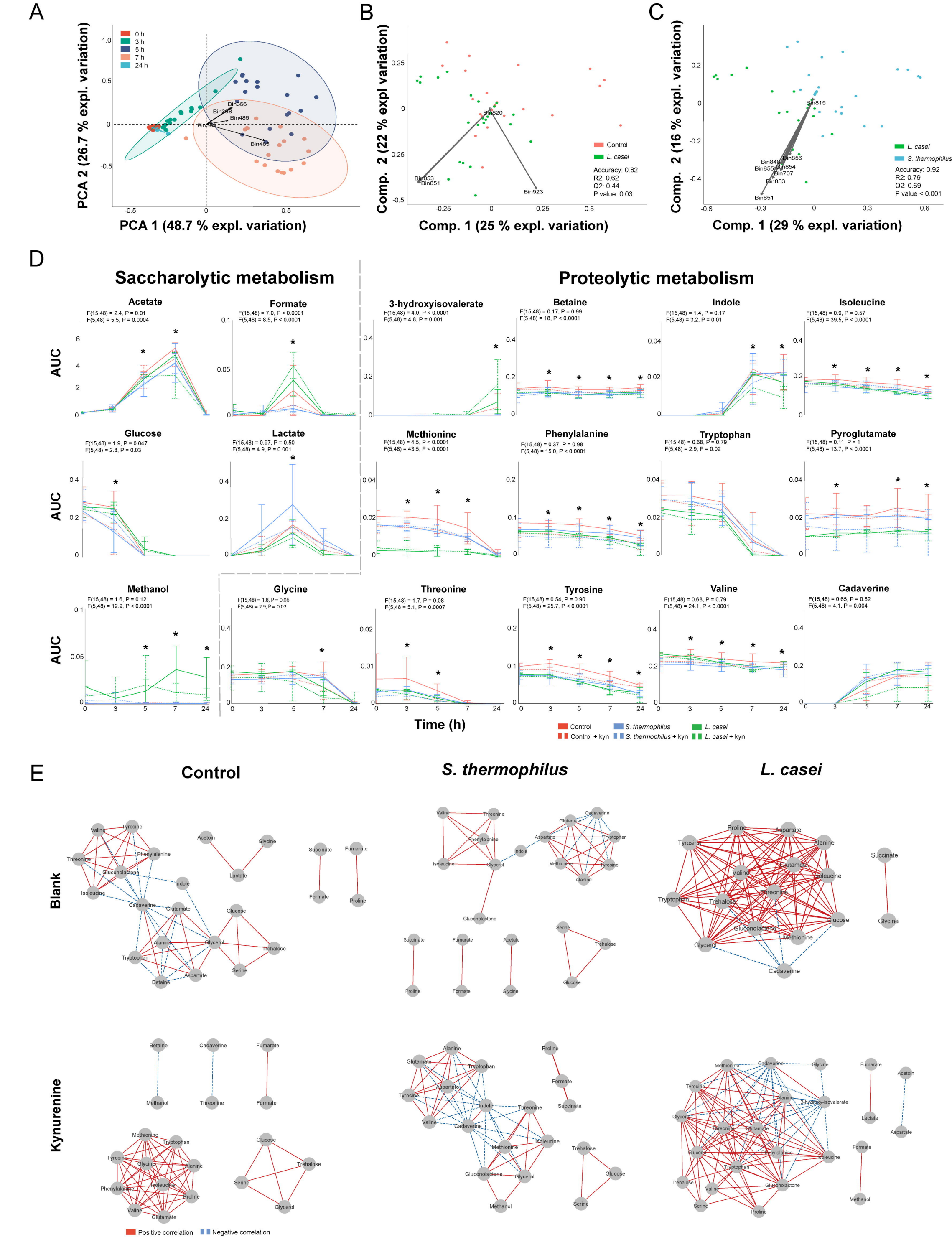
A
0 h
3 h
5 h
7 h
24 h
PCA 2 (26.7 % expl. variation)
PCA 1 (48.7 % expl. variation)
Bin366
Bin486
Bin455
B
Control
L. casei
Accuracy: 0.82
R2: 0.62
Q2: 0.44
P value: 0.03
Comp. 2 (22 % expl variation)
Comp. 1 (25 % expl. variation)
Bin820
Bin853
Bin851
Bin923
C
L. casei
S. thermophilus
Accuracy: 0.92
R2: 0.79
Q2: 0.69
P value < 0.001
Comp. 2 (16 % expl. variation)
Comp. 1 (29 % expl. variation)
Bin815
Bin856
Bin848
Bin855
Bin854
Bin707
Bin853
Bin851
D
Saccharolytic metabolism
Proteolytic metabolism
Acetate
F(15,48) = 2.4, P = 0.01
F(5,48) = 5.5, P = 0.0004
Formate
F(15,48) = 7.0, P < 0.0001
F(5,48) = 8.5, P < 0.0001
3-hydroxyisovalerate
F(15,48) = 4.0, P < 0.0001
F(5,48) = 4.8, P = 0.001
Betaine
F(15,48) = 0.17, P = 0.99
F(5,48) = 18, P < 0.0001
Indole
F(15,48) = 1.4, P = 0.17
F(5,48) = 3.2, P = 0.01
Isoleucine
F(15,48) = 0.9, P = 0.57
F(5,48) = 39.5, P < 0.0001
Glucose
F(15,48) = 1.9, P = 0.047
F(5,48) = 2.8, P = 0.03
Lactate
F(15,48) = 0.97, P = 0.50
F(5,48) = 4.9, P = 0.001
Methionine
F(15,48) = 4.5, P < 0.0001
F(5,48) = 43.5, P < 0.0001
Phenylalanine
F(15,48) = 0.37, P = 0.98
F(5,48) = 15.0, P < 0.0001
Tryptophan
F(15,48) = 0.68, P = 0.79
F(5,48) = 2.9, P = 0.02
Pyroglutamate
F(15,48) = 0.11, P = 1
F(5,48) = 13.7, P < 0.0001
Methanol
F(15,48) = 1.6, P = 0.12
F(5,48) = 12.9, P < 0.0001
Glycine
F(15,48) = 1.8, P = 0.06
F(5,48) = 2.9, P = 0.02
Threonine
F(15,48) = 1.7, P = 0.08
F(5,48 = 5.1, P = 0.0007
Tyrosine
F(15,48) = 0.54, P = 0.90
F(5,48) = 25.7, P < 0.0001
Valine
F(15,48) = 0.68, P = 0.79
F(5,48) = 24.1, P < 0.0001
Cadaverine
F(15,48) = 0.65, P = 0.82
F(5,48) = 4.1, P = 0.004
AUC
Time (h)
Control
Control + kyn
S. thermophilus
S. thermophilus + kyn
L. casei
L. casei + kyn
E
Control
S. thermophilus
L. casei
Blank
Kynurenine
Positive correlation
Negative correlation